J Radioanal Nucl Chem (2015) 304:517–525
DOI 10.1007/s10967-014-3879-2

Influences of planar source thickness on betavoltaics with different semiconductors

Yun-peng Liu · Xiao-bin Tang · Zhi-heng Xu · Liang Hong · Hao Wang · Min Liu · Da Chen

Received: 16 June 2014 / Published online: 14 January 2015

Abstract Employing ^{63}Ni and ^{147}Pm with different thicknesses and apparent activity densities, we calculated the total efficiency (η_{total}) and conversion efficiency (η) limits of betavoltaics by MCNP5 and Schottky equation. The apparent activity density, emitted average energy, and η limit increase and then reach their saturation levels with increasing source thickness. The increment rate of η limit increasingly smaller as the bandgap increases. Wide bandgap semiconductors lead η to reach saturation and η_{total} to reach maximum more quickly than narrow ones. The limit of η for ^{147}Pm is higher than that for ^{63}Ni. Measurement results demonstrate that high apparent activity density can improve η as expected. This study can serve as a reference to evaluate the performance of betavoltaics.

Keywords Efficiency limit · Betavoltaic · Different thickness · Apparent activity density · MCNP5

Introduction

As one kind of nuclear batteries, betavoltaics store energy in a beta source; that energy is converted to electricity when the beta particles interact with a semiconductor PN junction to create electron–hole pairs (EHPs) that are drawn off as current [1]. With long-lifetime, high-energy–density and amenable-to-miniaturization, betavoltaics possess significant potential for use as next-generation microbatteries in microelectromechanical systems [2]. They have become worldwide research and development hotspots [1, 3].

Energy conversion efficiency is one of important performance parameters of betavoltaics. There are usually two types of energy conversion efficiencies involved in betavoltaic studies. One is total efficiency (η_{total}), which refers to the ratio of the maximum output power (P_{max}) to the total power of the beta source. Another is conversion efficiency (η), which refers to the ratio of P_{max} to the energy of apparent emitted particles directed towards the energy conversion unit. Most of previous studies evaluate the performances of betavoltaics by simply comparing their efficiency values. However, this evaluation method is insufficient. The main reason is that the efficiency limits of betavoltaics are not constant under various source conditions, such as activity density and thickness, and semiconductor conditions, such as bandgap. There are several studies involved the influences of beta source and semiconductor conditions on the efficiency limits of betavoltaics. Rappaport [4] analyzed the effects of energy spectrum, source activity, bandgap, and so on. Short-circuit current and open-circuit voltage were assumed equal to the current and voltage at maximum output power. This assumption can overstate the efficiency limit, particularly at low activity. Wei [5] calculated the η_{total} of a Si betavoltaic as a function of ^{147}Pm total activity but did not consider the limit of η. Olsen [6] formulated the theory of betavoltaics and reported the limit of η as a function of bandgap.

Y. Liu · X. Tang (✉) · Z. Xu · L. Hong · H. Wang · M. Liu · D. Chen
Department of Nuclear Science and Engineering, Nanjing University of Aeronautics and Astronautics, Nanjing 210016, China
e-mail: tangxiaobin@nuaa.edu.cn

Y. Liu · X. Tang · Z. Xu · L. Hong · H. Wang · M. Liu · D. Chen
Jiangsu Key Laboratory of Material and Technology for Energy Conversion, Nanjing 210016, China

However, the η limit did not incorporate accurate transport models of beta particles.

Besides, most of previous experimental studies [7–9] obtain the value of η by using the average energy of source particles. Rappaport [4] and Li et al. [10] found that the emitted energy spectrum changes as the source thickness increases. The average energy of apparent emitted particles will be different from that of source particles due to self-absorption loss [11]. Although Wacharashindhu et al. [11] did not use the term "apparent activity density", and its concept was addressed as part of "self-absorption loss". However, limited information is available on the average energy of apparent emitted particles from sources with different thicknesses.

Therefore, we believe that it is important to further study the characteristics of the apparent emitted particles of the beta source and the influences of the source thickness, apparent activity density and emitted average energy on efficiency limits of betavoltaics. In this paper, we investigated the limits of η_{total} and η of betavoltaics irradiated by ^{63}Ni and ^{147}Pm with different thicknesses and apparent activity densities through MCNP5 and Schottky equation. The effect of the semiconductor bandgap on the efficiency limits of betavoltaics was also studied. The apparent activity density and emitted average energy were simulated in detail. To verify the theoretical effect of the apparent activity density on η, we fabricated a Si betavolatic and measured the output performance of the betavoltaic irradiated by ^{63}Ni with two different apparent activity densities. The measured η and P_{max} were compared with the calculated values. This study can serve as a reference to evaluate the performance of betavoltaics.

Materials and methods

Semiconductors and beta sources

Olsen [6] concluded that ^{3}H, ^{63}Ni, and ^{147}Pm are feasible betavoltaic sources. The end-point energy of these sources is low enough that the radiation effects in many semiconductors can be tolerated. In this study, we selected ^{63}Ni and ^{147}Pm as beta sources. Previous betavoltaic studies involved Si, Ge, GaAs, GaP, SiC, GaN, diamond, and selenium devices. The semiconductor materials studied in this paper are listed in Table 1.

Table 1 Semiconductors of betavoltaics

Semiconductors	Si	GaAs	GaP	4H-SiC	GaN	Diamond
Bandgap (eV)	1.12	1.43	2.26	3.26	3.4	5.5

Theoretical simulation model

As illustrated in Fig. 1, a source film model with a base area 1×1 cm^2 was established using MCNP5, and the exterior region of the beta source was set to vacuum. The isotopic abundance of ^{63}Ni and ^{147}Pm was set to 100 %. The densities of ^{63}Ni and ^{147}Pm are 8.09 and 7.22 g/cm^3. ^{147}Pm exists in the form of Pm_2O_3. The energy spectra of ^{63}Ni and ^{147}Pm originate from ICRP 38. The average energies of the energy spectra of ^{63}Ni and ^{147}Pm are 1.7154×10^{-2} and 6.2121×10^{-2} MeV, respectively. The thicknesses of ^{63}Ni and ^{147}Pm range from 0.01 to 20 and 0.01 to 200 μm, respectively.

With different source thicknesses, the number of beta particles emitted from the source surface was recorded by using a surface current tally with energy bins. The energy of the emitted particles was also recorded by using the same tally. During the simulation, there were two kind of apparent activity densities to be counted. One is 4π apparent activity density, which is defined as the activity density of all beta particles emitted from the six surfaces of the beta source. The other is both sides apparent activity density, which is defined as the activity density of all beta particles emitted from the top and bottom surfaces of the beta source. Based on these simulation results, apparent activity density, emitted energy spectrum, and emitted average energy were obtained, respectively. Besides, the total activity was deduced by physical parameters of the beta source, including the molar mass, density, based area, thickness, and half-lifetime [10].

Theoretical performance calculation

The apparent activity densities and emitted average energies of the beta sources with different thicknesses were simulated and obtained by above simulation source model. After that, the output performances, including the limits of η and η_{total} of the betavoltaics irradiated by those beta sources were calculated by Schottky equation as follows.

The total efficiency of the betavoltaic can be given by

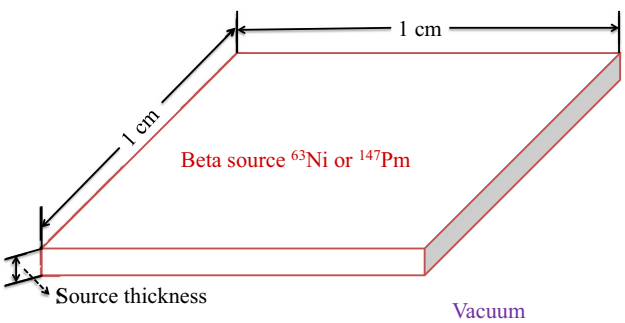

Fig. 1 Simulation geometry model of the beta source

$$\eta_{\text{total}} = \eta_\beta \Omega \eta \quad (1)$$

where η_β is the apparent emitted efficiency of beta particles and the solid angle Ω is the ratio of the number of particles directed towards the semiconductor to the number of particles emitted by the beta source. According to Eq. (1), the expressions "$1 - \eta_\beta$" and "$1 - \Omega$" can be defined as the self-absorption loss and directional loss, respectively [11]. The value of η can be expressed as

$$\eta = (1 - \mu)(1 - r)Q\eta_s \quad (2)$$

where μ, called the external interaction loss, is the radiation loss between the beta source and the active region of the betavoltaic by interactions with media, such as air and electrode; r is the reflection coefficient for beta particles from the semiconductor surface; Q is the collection efficiency of EHPs; and η_s is semiconductor efficiency, which refers to the ratio of $P_{\max}$ to the energy deposited in the energy conversion unit. According to Eq. (2), the expression "$1 - Q$" can be defined as the collection loss.

To obtain the maximum short-circuit current density (J_{sc} in A/cm^2) and the subsequent efficiency limits, we assume that all particles emitted from the beta sources are delivered into the semiconductor without directional loss, external interaction loss, reflection loss, and collection loss in the calculation. The value of J_{sc} can be written as

$$J_{sc} = qE_aA_a/E_{ehp} \quad (3)$$

where q indicates the quantity of electric charge by electron or hole (in C), E_a is the average energy of apparent emitted particles (in MeV), A_a is the apparent activity density (in mCi/cm^2), and E_{ehp} is the average energy needed to generate an EHP, which is given by

$$E_{ehp} = 2.8E_g + 0.5 \quad (4)$$

where E_g is the bandgap of the semiconductor material.

According to Shockley equation, the open-circuit voltage (V_{oc} in V) for an ideal PN junction betavoltaic can be expressed as

$$V_{oc} = kT/q \ln(J_{sc}/J_0 + 1) \quad (5)$$

where k indicates Boltzmann constant and J_0 is the minimum value of the reverse saturation current density (in A/cm^2), which can be expressed by [12]

$$J_0 = 1.5 \times 10^5 \exp(-E_g/kT) \quad (6)$$

Basing on the preceding assumptions, we can conclude that the limit of η equals that of η_s and is given by [6]

$$\eta = V_{oc}\text{FF}/E_{ehp} \times 100\ \% \quad (7)$$

where FF is the fill factor, which can be expressed as

$$\text{FF} = [\upsilon_{oc} - \ln(\upsilon_{oc} + 0.72)]/(\upsilon_{oc} + 1) \quad (8)$$

where υ_{oc} is the normalized open-circuit voltage, namely, $V_{oc}/kT/q$.

The total efficiency limit can be written as

$$\eta_{\text{total}} = P_{\max}S/E_tA_t \quad (9)$$

where $P_{\max}$ is the maximum output power density (in W/cm^2); S is the PN junction area (in cm^2), which is equal to the surface area of the beta source; E_t is the average energy of source particles (in MeV); and A_t is the total activity of the beta source (in mCi).

Fabrication and measurement

Phosphorus-doped Si substrate with 9.3×10^{13}/cm^3 was used in the experiment. The energy conversion unit of the betavoltaic was manufactured via BF_2^+ ion implantation and 30 min conventional thermal annealing. The implantation energy and implantation dose were 120 keV and 6×10^{14}/cm^2, respectively. To reduce the tunneling effect, a 30 nm-thick SiO_2 layer was grown on the front surface of Si via thermal oxidation prior to implantation. Thus, an energy conversion unit with a surface doping density of 1×10^{19}/cm^3 and a junction depth of 0.6 μm was successfully produced. The active area of the energy conversion unit was 0.5×0.5 cm^2.

Two ^{63}Ni sources for testing are both disc-shaped. Table 2 shows the specific parameters. The factory date of ^{63}Ni is August 11, 2011. The I–V characteristic of the betavoltaic was measured using a Keithley 2636A SourceMeter on January 23, 2013. The measured $P_{\max}$ was extracted from the I–V curve. The measured η was given by Eq. (10).

$$\eta = P_{\max}S/E_aA_a \quad (10)$$

where $P_{\max}$ refers to the measured $P_{\max}$; S is 0.25 cm^2; A_a is the apparent activity density in testing (Table 2); and E_a is the average energy of apparent emitted particles. After that, the measured η and $P_{\max}$ were compared with the calculated values.

Results and discussion

Simulated total activity and apparent activity density

The total activity and apparent activity density show similar responses to increasing ^{63}Ni and ^{147}Pm thicknesses

Table 2 Active diameter and apparent activity density of beta sources

Sources	Active diameter (mm)	Factory apparent activity density (mCi/cm^2)	Apparent activity density in testing (mCi/cm^2)
^{63}Ni	25	2	1.98
^{63}Ni	25	5	4.95

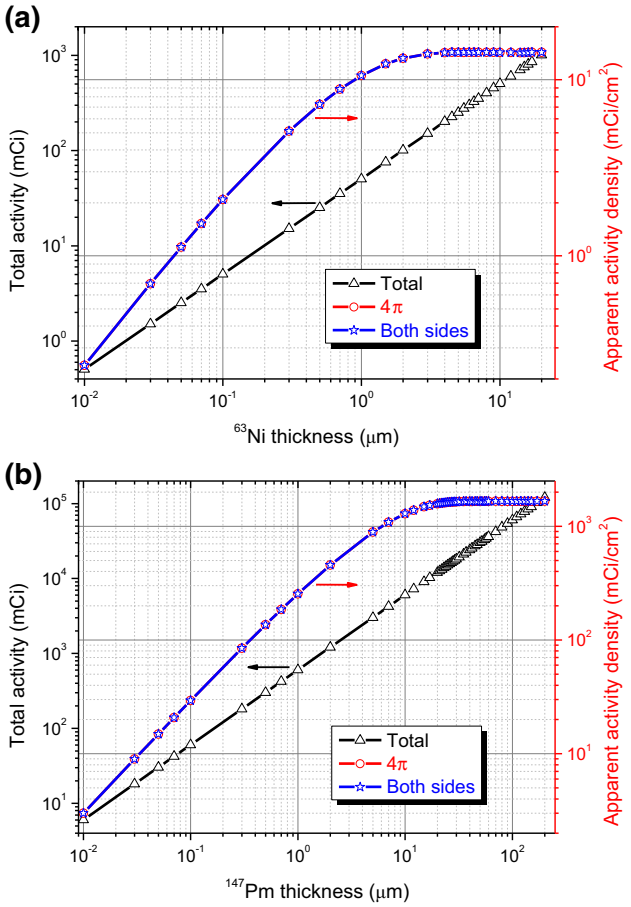

Fig. 2 Total activity and apparent activity density as a function of **a** ^{63}Ni and **b** ^{147}Pm thicknesses

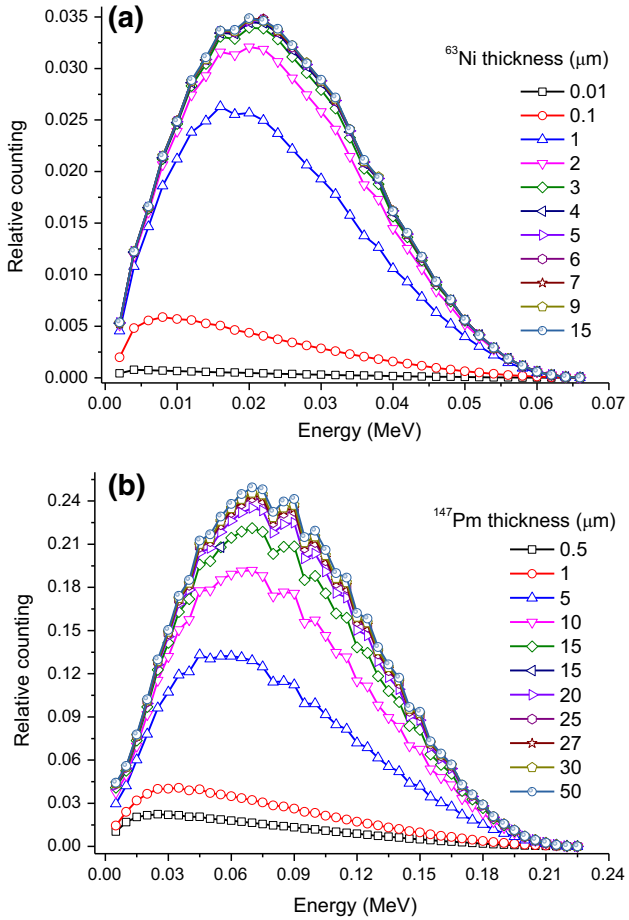

Fig. 3 Apparent emitted energy spectrum as a function of **a** ^{63}Ni and **b** ^{147}Pm thicknesses

(Fig. 2). The total activity linearly increases with increasing thickness. The apparent activity densities of 4π and both sides quickly increase, slowly increase, and then reach their saturation levels as the source thickness increases. These results can be attributed to the effect of self-absorption. Wacharasindhu et al. [11] presented similar MCNPX simulations that recorded the number of particles escaping a monoenergetic beta source of 1.67×10^{-1} MeV in relation to its thickness and base area. For ^{63}Ni in Fig. 2a, the saturation values of the apparent activity densities of 4π and both sides are 1.4340×10^{1} and 1.4342×10^{1} mCi/cm^2, respectively, at approximately 6 μm thickness. For ^{147}Pm in Fig. 2b, those two saturation values are 1.6407×10^{3} and 1.6424×10^{3} mCi/cm^2, respectively, at approximately 30 μm thickness.

In addition, as shown in Fig. 2, the 4π apparent activity density is quite close to the both sides one at the same source thickness. The following simulation and calculation results in this study are based on the 4π emitted particles.

Simulated emitted energy spectrum and emitted average energy

The shape of the apparent emitted energy spectrum is not fixed as the source thickness changes (Fig. 3). The peak of particle energy distribution moves towards the high-energy section in both cases of ^{63}Ni and ^{147}Pm. Similar behavior was demonstrated by ^{90}Sr–^{90}Y [4] and ^{3}H [10]. This phenomenon was due to the different penetrating powers of particles with different energies. As the emission location of source particles becomes deeper, high-energy particles have a greater likelihood of emitting from the source surface, and low-energy particles have a greater likelihood of being absorbed by the source itself. With increasing source thickness, the proportion of high-energy particles in the energy spectrum becomes increasingly large. However, when the source thickness is large enough, deep source particles, even high-energy particles, can barely emit from the source surface. This result indicates that the emitted energy spectrum remains unchanged. For ^{63}Ni (Fig. 3a), the curves from 4 to 15 μm are almost overlapping. For

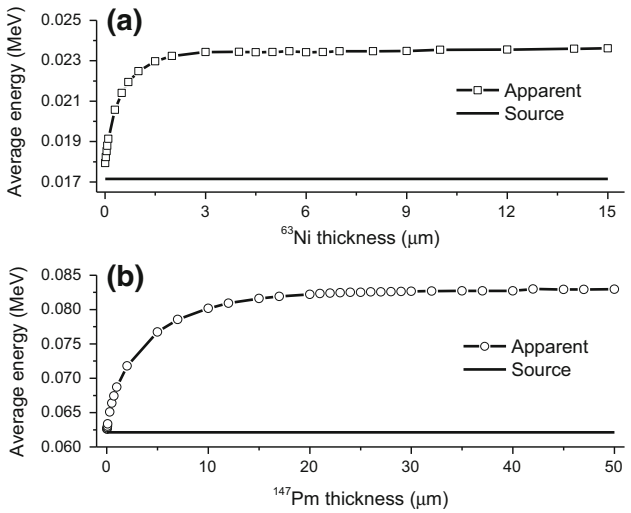

Fig. 4 Average energy of apparent emitted and source particles of **a** ^{63}Ni and **b** ^{147}Pm

^{147}Pm (Fig. 3b), the curves from 25 to 50 μm are almost overlapping.

It can be expected that the average energy of apparent emitted particles will change as the source thickness changes due to the variation in the emitted energy spectrum. As shown in Fig. 4a and b, the emitted average energy remarkably increases with increasing source thickness in both cases of ^{63}Ni and ^{147}Pm. The emitted average energy for ^{63}Ni exhibits the same trends as that for ^{147}Pm. As the source thickness increases, the emitted average energy rapidly increases, slowly increases, and then reaches the saturation value. This finding is consistent with the apparent emitted energy spectrum presented in Fig. 3.

Basing on the preceding analysis, we can conclude that the value of η calculated by the average energy of source particles is obviously overstated. The real average energy of apparent emitted particles should be employed to calculate η. The average energy can be evaluated using the theoretical method in this study or measured using a beta spectrometer.

Calculated efficiency limits

With ^{63}Ni and ^{147}Pm of different thicknesses, we calculated the efficiency limits of betavoltaics based on different semiconductors using the theoretical method. The limits of η_{total} and η both remarkably change as the source thickness increases (Fig. 5). η_{total} and η show similar responses to increasing thicknesses of ^{63}Ni and ^{147}Pm (Fig. 5a, b).

The term of FF is a function of υ_{oc}, where depends on the value of V_{oc}. Therefore, once a given semiconductor is selected, according to Eq. (8), the limit of η is only affected by V_{oc}. Take Si for example, a ^{63}Ni with a thickness of 0.1 μm and a consequent apparent activity density of 0.239 mCi/cm^2 can produce a J_{sc} with 6.995×10^{-9} A/cm^2. For Si, the value of J_0 is 2.296×10^{-14} A/cm^2. In this case, the ratio of J_{sc}/J_0 is about 3.05×10^5, which is considerably larger than 1. When J_{sc} is much greater than J_0, the Eq. (5) could be written as:

$$V_{\text{oc}} \approx \frac{kT}{q}\ln\left(\frac{aXJ'_{\text{sc}}}{J_0}\right) = \frac{kT}{q}\ln\left(\frac{J'_{\text{sc}}}{J_0}\right) + \frac{kT}{q}\ln aX = V'_{\text{oc}} + \frac{kT}{q}\ln aX \quad (11)$$

where J'_{oc} and V'_{oc} is the short-circuit current density and open-circuit voltage produced by a 1 mCi/cm^2 beta source with a certain thickness, X is a number which equals the value of the apparent activity density of the beta source with a certain thickness, the term of a is the ratio of the emitted average energy of the X mCi/cm^2 beta source and that of the 1 mCi/cm^2 beta source, and V_{oc} is the open-circuit voltage produced by the X mCi/cm^2 beta source with a certain thickness. By the beta source model shown in Fig. 1 or the data shown in Fig. 2, it can be known that the 1 mCi/cm^2 ^{63}Ni and 1 mCi/cm^2 ^{147}Pm correspond to the 0.0445 μm ^{63}Ni and 0.0034 μm ^{147}Pm, respectively. Accordingly, the emitted average energies of ^{63}Ni and ^{147}Pm are 1.8443×10^{-2} and 6.2329×10^{-2} MeV (Fig. 4a, b). Table 3 shows the values of V_{oc}' of betavoltaics irradiated by 1 mCi/cm^2 ^{63}Ni with 0.0445 μm and 1 mCi/cm^2 ^{147}Pm with 0.0034 μm, respectively. For ^{63}Ni, when the source thickness increases from 0.01 μm to the saturation thickness 6 μm, the range of a is 0.930–1.270. For ^{147}Pm, when the source thickness increases from 0.01 μm to the saturation thickness 30 μm, the range of a is 1.001–1.326.

As shown in Fig. 5, the value of η rapidly increases, slowly increases, and then reaches the saturation value as the source thickness increases. The trend of the emitted average energy and the apparent activity density can be used to explain this phenomenon. Once a given semiconductor is selected, J_{sc} is a function of the emitted average energy and the apparent activity density. Because V_{oc} is a function of J_{sc}, the limit of η becomes a function of the emitted average energy and the apparent activity density. When the source thickness increases, the values of a and X in Eq. (11) rapidly increases, V_{oc} and the consequent η limit rapidly increase. Then, when the source thickness continues to increase, the values of a and X slowly increases, V_{oc} and the consequent η limit slowly increase. Finally, when the source thickness increases to the saturation level, the values of a and X reach their saturation values, V_{oc} and the consequent η limit reach their maximum value approximately.

On the one hand, when the source thickness and the consequent apparent activity density changes, different semiconductors have the same a and X. This phenomenon

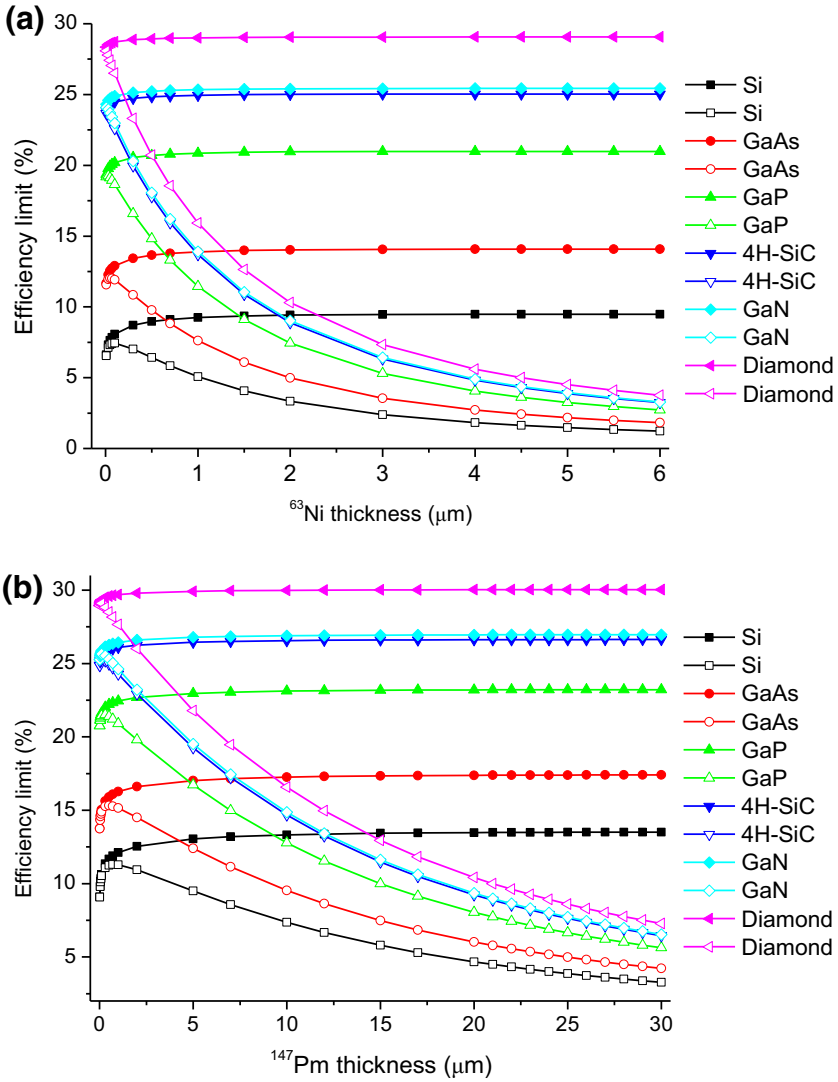

Fig. 5 Efficiency limits of betavoltaics based on different semiconductors as a function of the thicknesses of **a** ^{63}Ni and **b** ^{147}Pm *Solid symbol*—the limit of η; *Open symbol*—the limit of η_{total}

Table 3 Values of V'_{oc} of betavoltaics irradiated by 0.0445 μm, 1 mCi/cm^2 ^{63}Ni and 0.0034 μm, 1 mCi/cm^2 ^{147}Pm respectively

Semiconductors	V'_{oc}(V)	
	0.0445 μm, 1 mCi/cm^2 ^{63}Ni	0.0034 μm, 1 mCi/cm^2 ^{147}Pm
Si	0.3643	0.3961
GaAs	0.6687	0.7005
GaP	1.4880	1.5198
4H-SiC	2.4791	2.5109
GaN	2.6181	2.6498
Diamond	4.7061	4.7379

indicates that the second item on the left side of Eq. (11), that is the increment of V_{oc}, is the same for any semiconductors. On the other hand, the wide bandgap semiconductor has lower J_0 than the thin one. This phenomenon indicates that the first item on the left side of Eq. (11) for the wide bandgap semiconductor is larger than that for the thin one (Table 3). Hence, the wide bandgap semiconductor has low increment rate of V_{oc}. As a result, the increment rate of η limit increasingly smaller as the bandgap increases. Table 4 shows the limits of η of betavoltaics irradiated by thin and thick source films and the corresponding increment rates.

It can also be seen in Fig. 5 that the wide bandgap semiconductor allows η to reach the saturation value more

Table 4 Limits of η of betavoltaics with thin and thick source films and the corresponding increment rates

Semiconductors	η (%)		Increment rate (%)	η (%)		Increment rate (%)
	0.01 μm ^{63}Ni	6 μm ^{63}Ni		0.01 μm ^{147}Pm	30 μm ^{147}Pm	
Si	6.61	9.48	43.42	9.09	13.51	48.62
GaAs	11.68	14.08	20.55	13.76	17.41	26.57
GaP	19.36	20.98	8.37	20.77	23.22	11.80
4H-SiC	23.88	25.04	4.86	24.88	26.63	7.03
GaN	24.32	25.43	4.56	25.28	26.96	6.65
Diamond	28.36	29.06	2.47	28.97	30.03	3.66

quickly than the narrow one as the source thickness increases, although the narrow bandgap semiconductor has high η increment rate. The value of J_0 is responsible for this result. Compared with the narrow bandgap semiconductor, the wide one with ultralow J_0 makes V_{oc} and the subsequent η limit closer to their maximum values at thin source thickness and low apparent activity density.

The limit of η_{total} rapidly reaches the maximum value and then declines with increasing source thickness. The source thickness with respect to the maximum η_{total} based on the wide bandgap semiconductor is smaller than that based on the narrow one. For example, the limit of η_{total} reaches the maximum value of 7.45 % at 0.1 μm for Si and 23.66 % at 0.01 μm for GaN in the case of ^{63}Ni. The value of J_0 and the trend of η limit are responsible for this result.

In addition, when the thickness of the beta source remains the same, the limits of η_{total} and η of the betavoltaic based on the wide bandgap semiconductor are respectively larger than those based on the narrow one.

To study the influence of the type of the beta source on the limit of η of the betavoltaic, we set the apparent activity densities of ^{63}Ni and ^{147}Pm to the same order of magnitude. By converting the horizontal ordinate in Fig. 5, that is the source thickness, into the apparent activity density, the limit of η of the betavoltaic with different types of beta sources was obtained and shown in Fig. 6. Once a given

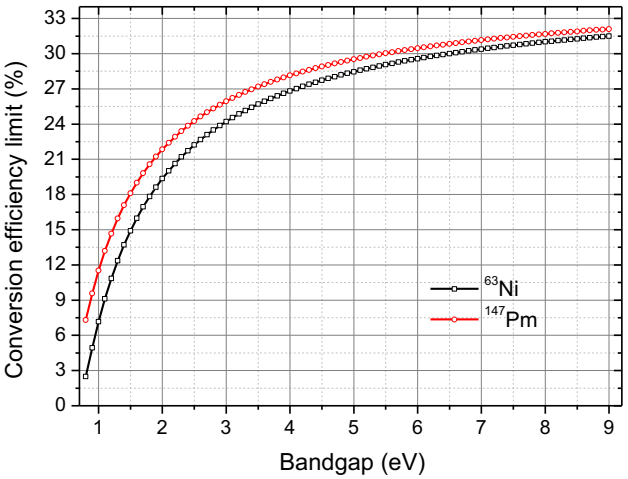

Fig. 7 Limit of η as a function of bandgap

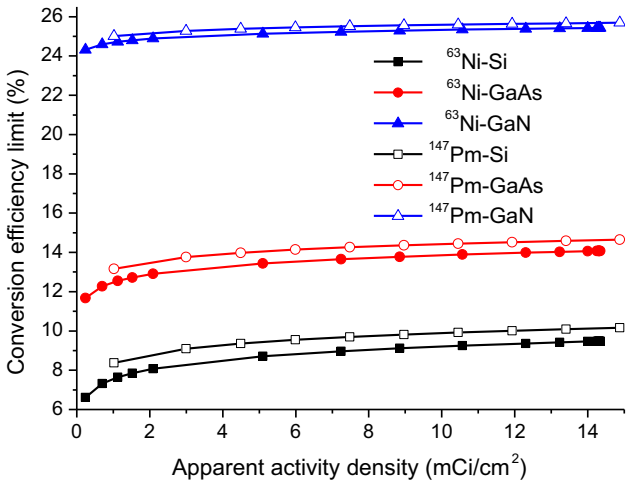

Fig. 6 Limit of η of the betavoltaic with different types of beta sources

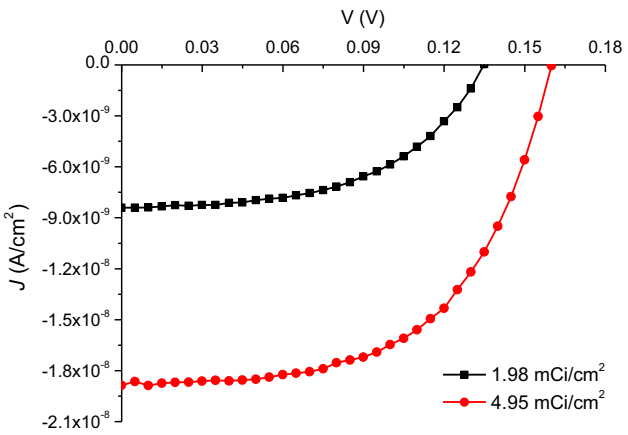

Fig. 8 Measured *I–V* characteristics of betavoltaics based on ^{63}Ni of different apparent activity densities

Table 5 Measured and calculated performances of the betavoltaics

Sources	Estimated source thickness (μm)	Emitted average energy (MeV)	Measured values		Calculated values	
			P_{max} (W/cm^2)	η (%)	P_{max} (W/cm^2)	η (%)
1.98 mCi/cm^2 ^{63}Ni	0.095	1.9074×10^{-2}	5.95×10^{-10}	0.27	1.82×10^{-8}	8.03
4.95 mCi/cm^2 ^{63}Ni	0.293	2.0532×10^{-2}	1.72×10^{-9}	0.29	5.30×10^{-8}	8.68

semiconductor is selected, the values of E_{ehp} and J_0 remain unchanged. When the apparent activity density is constant, the J_{sc} and the subsequent V_{oc} and FF increase with the increasing of the emitted average energy. This result will lead to high η limit. Although the thickness of ^{63}Ni and densities is different from that of ^{147}Pm with the same apparent activity, the emitted average energy of ^{147}Pm is larger than that of ^{63}Ni. Therefore, it can be seen in Fig. 6 that the limit of η of the betavoltaic irradiated by ^{147}Pm is higher than that by ^{63}Ni with the same apparent activity density for Si, GaAs, and GaN respectively. Beyond that, Fig. 6 intuitively shows that the η limit increases as the apparent activity density increases. The reasons for this result have been stated above.

To study the influence of the bandgap on the limit of η of the betavoltaic with the limit source condition, we set the thicknesses of ^{63}Ni and ^{147}Pm to their saturation values of 6 and 30 μm respectively. And then the limit of η as a function of bandgap was calculated (Fig. 7). The limit of η increases with increasing bandgap, which agrees well with the findings of Olsen [6]. Besides, the limit of η based on ^{63}Ni is lower than that based on ^{147}Pm for the same bandgap. This result can be attributed to two reasons. First, the apparent activity density of ^{147}Pm with 30 μm is larger than that of ^{63}Ni with 6 μm. Second, the emitted average energy of ^{147}Pm is higher than that of ^{63}Ni.

The preceding results and analysis indicate that the conditions of sources and semiconductors should be considered when the values of η are compared. The performance of betavoltaics may be evaluated by comparing the difference between the measured and calculated η.

Comparison of measured and calculated efficiencies

Figure 8 shows the measured *I–V* characteristics of betavoltaics irradiated by 1.98 and 4.95 mCi/cm^2 ^{63}Ni, respectively. The J_{sc} and V_{oc} of the betavoltaic are obviously improved with the beta source of high apparent activity density.

Table 5 shows the measured and calculated performances of the betavoltaics. The source thickness, emitted average energy, and the subsequent η in Table 5 were approximately estimated from data shown in Figs. 2a, 4a, and 6 based on the factory parameters of beta sources in Table 2, respectively. As expected from the calculation results, the measured η and P_{max} of the betavoltaic irradiated by the high apparent activity density ^{63}Ni are respectively higher than those of the betavoltaic irradiated by the low apparent activity density ^{63}Ni. However, there are still large gap between the measured and calculated values. This result is contributed to several efficiency losses, including external interaction loss, reflection loss, and collection loss.

Conclusions

We determined the limits of η_{total} and η of betavoltaics based on semiconductors with different bandgaps irradiated by ^{63}Ni and ^{147}Pm with different thicknesses and apparent activity densities through MCNP5 and Schottky equation. Simulation results show that apparent activity density and emitted average energy rapidly increase, slowly increase, and then reach their saturation values as the source thickness increases. Calculation results show that the limit of η rapidly increase, slowly increase, and then reach the saturation value as the source thickness increases. The increment rate of η limit increasingly smaller as the bandgap increases. The limit of η_{total} rapidly reaches the maximum value and then declines with increasing source thickness. Wide bandgap semiconductors lead η to reach saturation and η_{total} to reach maximum more quickly than narrow ones. The limit of η for ^{147}Pm is higher than that for ^{63}Ni with the same or saturation apparent activity density. The measurement results demonstrate that high apparent activity density can improve the value of η as the calculation results expected. This paper can serve as a reference for evaluating the performance of betavoltaics.

Acknowledgments This work was supported by the National Natural Science Foundation of China (Grant No. 11205088), the Aeronautical Science Foundation of China (Grant No. 2012ZB52021), the Natural Science Foundation of Jiangsu Province (Grant No. BK20141406), and the Priority Academic Program Development of Jiangsu Higher Education Institutions.

References

1. Olsen LC, Cabauy P, Elkind BJ (2012) Betavoltaic power sources. Phys Today 65(12):35–38
2. Chen C-C, Chang Y-Y, Zhang J-W (2012) A novel betavoltaic microbattery based on SWNTs thin film-silicon heterojunction.

In: Micro electro mechanical systems (MEMS), 2012 25th international conference on. IEEE, Paris, 2012, pp 1197-1200
3. Luo S-Z, Wang G-Q, Zhang H-M (2011) Advance in radiation-voltaic isotope battery. J Isot 24(1):3–13. doi:10.7538/tws.2011.24.01.0001
4. Rappaport P, Loferski JJ, Linder EG (1956) The electron-voltaic effect in germanium and silicon p-n. junctions. RCA Rev 17:100–134
5. Wei LS (1975) Parametric studies and optimization of the beta-voltaic cell—II open-circuit voltage and power efficiencies. Solid-State Electron 18(1):71–77
6. Olsen LC (1993) Review of betavoltaic energy conversion. In: Proceedings of the 12th space photovoltaic research and technology conference, Washington State University, 1993, pp 256–267
7. Guo H, Yang H, Zhang Y (2007) Betavoltaic micro batteries using porous silicon. In: Proceedings of the 20th IEEE micro electro mechanical systems, Japan Kobe, 2007, pp 867–870
8. Li X-Y, Ren Y, Chen X-J, Qiao DY-, Yuan W-Z (2011) ^{63}Ni schottky barrier nuclear battery of 4H-SiC. J Radioanal Nucl Chem 287(1):173–176
9. Cheng Z-J, San H-S, Chen X-Y, Liu B, Feng Z-H (2011) Demonstration of a high open-circuit voltage GaN betavoltaic microbattery. Chin Phys Lett 28(7):078401
10. Li H, Liu Y, Hu R, Yang Y-Q, Wang G-Q, Zhong Z-K, Luo S-Z (2012) Simulations about self-absorption of tritium in titanium tritide and the energy deposition in a silicon Schottky barrier diode. Appl Radiat Isot 70(11):2559–2563
11. Wacharasindhu T, Nullmeyer BR, Kwon JW, Robertson JD, Garnov AY (2014) Mechanisms leading to losses in conventional betavoltaics and evolution utilizing composite semiconductor with infused radioisotope for efficiency improvement. J Microelectromech S 23(1):56–65
12. Green MA (1982) Solar cells: operating principles, technology and system applications. Prentice-Hall, Englewood Cliffs